

# CNN based fault event classification and power quality enhancement in hybrid power system

Abdul Quawi<sup>1</sup>, Y. Mohamed Shuaib<sup>1</sup>, M. Manikandan<sup>2</sup>

<sup>1</sup>Department of Electrical and Electronics Engineering, B. S. Abdur Rahman Crescent Institute of Science and Technology, Chennai, India

<sup>2</sup>Department of Electrical and Electronics Engineering, Jyothishmathi Institute of Technology and Science, Telangana, India

## Article Info

### Article history:

Received Aug 26, 2023

Revised Feb 29, 2024

Accepted Mar 28, 2024

### Keywords:

Boost converter

CFLC

CNN

DWT

PV system

WECS

## ABSTRACT

A resilient approach is presented in this study for detecting and classifying faults for power distribution systems integrating renewable energy sources (RES). Combining discrete wavelet transform (DWT) and convolutional neural network (CNN). The suggested framework addresses the challenges of RES intermittency and kinetic energy insufficiency. The recommended methodology is evaluated in a MATLAB platform, featuring a power distribution system with photovoltaic (PV) and wind energy conversion system (WECS), stabilized by a boost converter and cascaded fuzzy logic controller (CFLC) based maximum power point tracking (MPPT) for PV and a PI controller for WECS. Comparative analyses demonstrate the superior performance of the CNN classifier with an accuracy of 96.33%, outshining existing classifiers, including ANN. Furthermore, under various fault conditions, the CNN consistently achieves high accuracy, with 98% for Islanding, 95% for line-to-ground fault, and 96% for line-to-line fault. The proposed approach exhibits excellent computational efficiency, with a training time of 10.5 hours, inference speed of 5 milliseconds, and resource utilization of 85%, emphasizing its suitability for instantaneous fault identification in power systems.

This is an open access article under the [CC BY-SA](https://creativecommons.org/licenses/by-sa/4.0/) license.



## Corresponding Author:

Y. Mohamed Shuaib

Department of Electrical and Electronics Engineering

B. S. Abdur Rahman Crescent Institute of Science and Technology

Chennai, Tamilnadu, India

Email: mdshuaiby@crescent.education

## 1. INTRODUCTION

The growing concerns regarding global warming and environmental pollution have accentuated the significance of RES based power production. According to International Renewable Energy Agency (IRENA), for year 2020, the capacity of world renewable energy has expanded by more than 260 GW, which is actually 50% greater than the amount of energy generated in 2019 [1], [2]. Among the available renewable energy sources (RES), the wind and solar energy account for a significant portion in terms of utilization rates. However, both these RES are characterized with intermittency, which leads to the introduction of electrical disturbances that distorts the current and voltage, resulting in several power quality disturbances (PQD). The massive infusion of power electronic technologies, which are non-linear in nature, into the electric power system has also resulted in the onset of serious PQD [3], [4]. These PQD has to be minimized in order to curtail power losses and also to prevent the malfunctioning of components interfaced to power system. The power grid faults are unpredictable and random in nature, hence the development of a precise and accurate fault detection technique is instrumental in ensuring its safe functioning. Moreover, for maintaining balance in power system,

a rapid fault detection model is essential as it improves the chances of quick recovery of unhealthy phases. Thus, by restoring the unhealthy phases, the stability, PQ and transient response of the entire power system is improved [5]-[10].

Numerous fault detection models for power distribution system are proposed so far, which includes a communication-based protection plan in [11] that offers a back-up security in case of absence of the main protection approach. In [12], the fault types in the output of the distributed generations are detected using abc to dq transformation. However, the protection technique proposed in these works concentrate only on a specific system topology or operating mode. A harmonic current based power distribution system protection plan is proposed in [13], while a zero and positive sequence voltage magnitude and phase angle-based fault detection approach is suggested in [14]. Due to the fluctuating fault impedances and dynamic load behaviour, it is a challenging task to establish a suitable threshold value in the aforementioned techniques. Recently, the neural network-based fault detection techniques are becoming increasingly popular. In these techniques, the various types of faults are identified by extracting the line signal's fault features as it is impossible to detect fault from unprocessed current or voltage signal. Some of commonly used signal processing tool for extracting features of the fault signals are Hilbert-Huang transform [15], S-transform [16] or wavelet transform [17].

For classifying the faults, machine learning techniques like support vector machines (SVM), k-nearest neighbours (k-NN) and decision trees (DT) are utilized [18], [19]. However, the data reduction method employed for minimizing the computational complexity, comes at the cost of information loss and lowered accuracy. A fault discernment mechanism is envisioned on the basis of artificial neural network (ANN) is suggested in [20], [21], while another fault discernment mechanism envisioned on the basis of probabilistic neural network (PNN) is suggested in [22]. The process of image classification is challenging in case of ANN, since the 2D images are required to be converted to 1D vectors, whereas the PNN are highly susceptible to input data discrepancies. RNN is also employed in grid connected solar systems but is susceptible to stability issues [23]. The most effective neural network for image classification is CNN and it is capable of handling large input image database. A comprehensive examination of contemporary methodologies introduced for the diagnosis of faults in power systems is elucidated within Table 1. The existing techniques provide valuable contributions to fault diagnosis in power systems, but there is a notable research gap that the proposed work aims to address. Specifically, none of the contemporary techniques discuss explicitly to integrate the advantages of both DWT and CNN for fault identification in a power distribution system that includes RES such as WECS and PV. This integration is precisely tailored to address the challenges posed by RES intermittency by employing separate stabilization methods for PV and WECS.

The contributions of the proposed methodology are:

- i) Integration of DWT and CNN: The proposed work introduces a novel fault detection methodology by combining the strengths of DWT for efficient feature extraction and CN for robust classification. This integration enhances the fault detection system's accuracy and effectiveness;
- ii) Addressing challenges in RES integration: The work specifically addresses challenges associated with the growing penetration of RES in power distribution systems. It recognizes and tackles issues such as RES intermittency, kinetic energy insufficiency, and the lack of zero crossing current, which are prime aspects of hybrid power system fault identification;
- iii) Comprehensive power system model: The proposed framework comprises a comprehensive power distribution system that includes both WECS and PV systems. The stability of each system is ensured through the use of specific control methodologies, such as the boost converter and CFLC for PV and the PI controller for WECS;
- iv) Holistic evaluation of power system: The proposed work goes beyond fault detection and includes a thorough evaluation of the power distribution system. It considers PQ issues, load variations, and influence of faults on entire system stability. This holistic approach provides a more complete understanding of the system's behavior under different conditions; and
- v) Simulation and transparency: Simulation outcomes are presented and evaluated using MATLAB platform, providing transparency and reproducibility. Thus, the proposed work contributes significantly to fault diagnosis in power distribution by introducing an integrated approach, addressing challenges in RES integration, providing a comprehensive power system model, conducting transparent simulations, performing a comparative analysis, and demonstrating the feasibility and efficiency of the proposed methodology.

These contributions collectively advance the understanding and application of fault detection techniques within the framework of contemporary power systems.

The subsequent sections of the paper are meticulously organized to present a coherent and comprehensive exploration of recommended fault identification system. Section 2 delves into materials and methods employed in the study, providing a detailed account of the working methodology. Section 3 outlines the intricacies of the proposed system, while the modeling intricacies of recommended system are expounded

upon in section 4 section 5 is dedicated to presenting the results and engaging in a thorough discussion. Simulation outcomes, parameters, and waveforms are meticulously analyzed to showcase efficacy of the envisioned fault identification approach under various fault conditions. Finally, section 6 encapsulates the findings and insights into a succinct conclusion.

Table 1. Contemporary techniques for fault diagnosis in power systems: an elaborate analysis

Ref.	Classifier/technique	Feature extraction	Strong points	Shortcomings
[24]	DT classifier	Hilbert Huang and empirical mode decomposition	Fast and accurate fault detection, classification, and location	Sensitivity to measurement quality, DG capacity changes, and fault incidence angles
[25]	Random forest (RF)	The technique used is not explicitly mentioned	High accuracy, robust generalization and effectual handling of missing data	Sensitive to noisy data and interpretability limitations
[26]	k-NN based ensemble classifier	DWT	Robust feature extraction by DWT and high discrimination accuracy	Multiple base classifiers introduce computational complexity
[27]	Genetic algorithm based ensemble classifier	Lasso penalty	Automatic fault diagnosis and uses less training dataset	Assumption of homogenous fault characteristics and limited dataset diversity
[28]	DT classifier	DWT	High impedance fault diagnosis and high classification accuracy	Performance under unpredictable noise require validation
[29]	Fuzzy neural network (FNN)	The technique used is not explicitly mentioned	Distributed processing, successful fault diagnosis and selective activation	Complex and resource intensive
[30]	Temporal constrained fuzzy petri nets	No feature extraction	Uncertainty integration, temporal constraints incorporation, feasibility and matrix algorithm	Challenges in adapting to highly dynamic power systems

## 2. MATERIALS AND METHODS

### 2.1. Dataset and simulation platform

The proposed fault detection system is evaluated using a simulated dataset generated on the MATLAB platform. The dataset includes voltage and current signals from a hybrid power system consisting of WECS and PV sources. These signals are recorded during normal operating conditions and under various fault scenarios.

### 2.2. Data pre-processing

Prior to training the CNN, the dataset undergoes pre-processing to ensure uniformity and relevance. This includes normalization of signal amplitudes, removal of noise, and segmentation of data into fault and non-fault instances. In order for the network to generalize patterns from the input signals, the pre-processing stage is essential.

### 2.3. CNN architecture

It is designed to efficiently capture spatial and temporal features from the fault signals. Its intricate design executes meticulous feature extraction using convolutional layers, dimensionality mitigation using max-pooling layers, classification using fully connected layers, and a softmax layer devoted to precise probability estimation. The training regimen is orchestrated through the employment of Backpropagation, leveraging stochastic gradient descent as the optimization algorithm, ensuring the network learns and refines its parameters effectively.

### 2.4. DWT feature extraction

Fault signal processing involves extracting relevant features using DWT. The voltage and current signals during fault condition onset are sensed and fed into DWT, which decomposes signals into approximation (App) and detail (Det) coefficients. These coefficients represent large and small scale frequency components, providing valuable information for fault classification.

### 2.5. CFLC MPPT

For the PV system, a boost converter with CFLC MPPT is employed to maximize power generation. The CFLC is configured with if-then rules based on inputs such as solar irradiance, temperature, voltage, current, and power. The cascading approach in the FLC helps reduce rule base complexity, ensuring efficient and precise MPPT under varying operating conditions.

## 2.6. Simulation parameters

Simulations are conducted with specified parameters. These parameters ensure a realistic representation of the hybrid power system and fault scenarios. The proposed fault detection system is assessed for its capability for precisely identifying and classifying various anomalies occurring in hybrid power system. The CNN classifier's effectiveness, coupled with DWT feature extraction and CFLC MPPT, is analysed based on simulation results and performance metrics such as accuracy, sensitivity, and specificity.

## 3. PROPOSED SYSTEM DESCRIPTION

The electrical power system in general encompasses numerous dynamic and interrelated components, which are highly liable to electrical faults. The stability and dependability of the electrical distribution system are negatively impacted by these failures, which can cause sizable financial losses. So, these faults are required to be detected and cleared immediately after their occurrence. A CNN classifier based fault event detection approach as seen in Figure 1 is envisioned in the recommended study. Moreover, the recommended fault detection approach is applied in a hybrid power system comprising of RES such as WECS and PV. Recently, the implementation of RES for power generation is becoming more popular on account of dwindling fossil fuel supply and increasing environmental pollution. However, the rise in integration of RES to the power system also causes serious protection risks in the power system. This is mainly attributable to their intermittent and variable nature, so with the intension of stabilizing their outputs, individual control methodologies are adopted. The PV system being the generator of low voltage supply, is coupled with a boost converter for enhancing its output voltage. Moreover, utmost power from PV is extracted with the assistance of CFLC MPPT.

The DFIG output is meticulously conveyed to PWM rectifier, a critical component in the system architecture. This rectifier plays a pivotal role in transforming the generated output into a stable DC form. Facilitating this transformation is the employment of a PI controller, adding a layer of precision and control to the stabilization process. Through a three phase VSI, the grid is linked to both of these distributed generators. The voltage signals of the system and current are monitored constantly, to discern fault occurrence. In case of a fault occurrence, faulty are sensed and sent as input to DWT, which in turn extracts the prominent features of the signal. Based on these extracted features, the CNN classifier instantly detects and classifies the type of the incurred fault. By detecting faults quickly, appropriate maintenance measures are taken to ensure power system reliability by preventing the onset of PQDs.

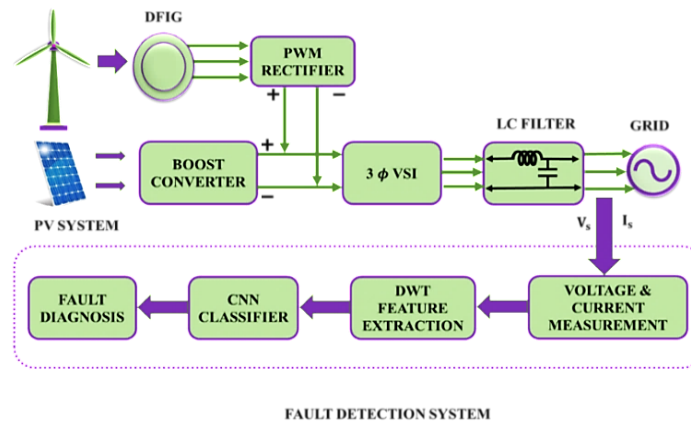


Figure 1. Architecture of CNN based fault detection model in a hybrid power system

## 4. PROPOSED SYSTEM MODELLING

### 4.1. Network fault types

The various faults that occur in a power line of power distribution system are classified broadly as series and shunt faults. The former is a result of series impedance imbalance caused due to plain break in one or two conductors. While, latter frequently occurs in a three-phase power network during distribution of power in the form of phase to ground (PG), phase-to-phase (PP), three PG (3 PG), and two PG (2 PG).

#### 4.1.1. Single PG fault

This short circuit fault takes place when a specific phase line drops to ground or comes in contact to neutral line. Moreover, it is caused due to falling of trees to the ground or as consequence of heavy rain. This can lead to an imbalance in the system, causing a surge in current flow through the grounded phase. The faulted

phase experiences a short circuit to the ground, resulting in an increase in current and potential overheating of equipment. Figures 2(a)-2(c) illustrates three types of single PG faults.

**4.1.2. Two PG fault**

This fault occurs due to the falling of two lines to the ground and it gives to fault current of higher magnitude. The simultaneous grounding of two phases creates a more significant imbalance in the system, leading to an increased flow of current through the faulted phases. This fault if not fixed immediately, develops a severe three-line to-the ground fault. Various types of two PG fault with fault resistance specified as  $R_f$  are displayed in Figures 2(d)-2(f).

**4.1.3. PP fault**

In a three-phase system, the PP fault occurs when there is a short circuit between two specific lines. The fault impedance magnitude of this unsymmetric fault, fluctuates over a wide range making it a challenging task to determine its lower and upper limits. In this fault scenario, two phases of the system become directly connected, bypassing the load impedance and creating an unintended low-impedance path for current flow between them. This can lead to an imbalance in the system, causing changes in voltage and current magnitudes. Figures 2(g)-2(i) illustrates the types of PP faults.

**4.1.4. Three PG fault**

It is a symmetric fault that often occurs and is caused because of equipment failure or falling of the electric pole. Moreover, it generates higher amount of short circuit current and the three-phase voltage becomes zero during this fault. During a three-phase fault, a substantial amount of short circuit current is generated because all three phases are directly connected, bypassing the impedance of the system. This fault condition causes a rapid increase in current magnitude, potentially leading to overheating of equipment and posing a significant threat to the integrity of the power system. Figure 2(j) illustrates this fault.

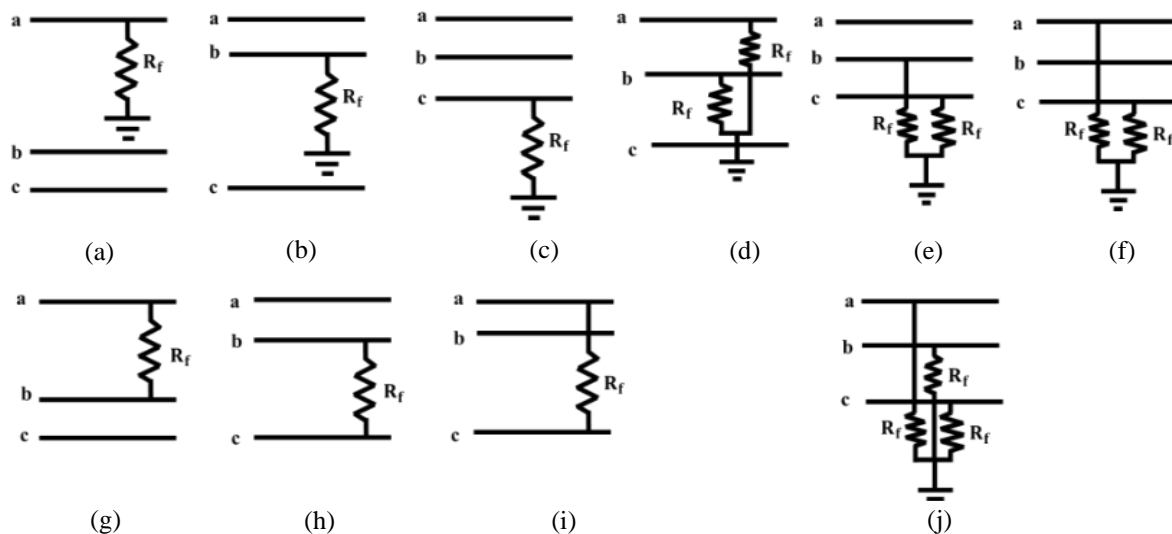


Figure 2. Types of faults: (a) a-g, (b) b-g, (c) c-g, (d) ab-g, (e) bc-g, (f) ca-g, (g) a-b, (h) b-c, (i) a-c, and (j) abc-g

**4.2. DWT based feature extraction of fault signals**

Voltage and current signals of the system during fault condition, are sensed and then provided as input to the DWT, which subsequently analyses the signal to identify its distinct features. It aids with the representation of signal in time domain as a collection of adjustable wavelet coefficients, which are capable of generating wide variety of signal processing effects. By representing the signals in different domain, better understanding of prominent features of the signal such as power spectrum, autocorrelation and periodicity is obtained. Here, during the occurrence of fault, the distinct feature of a fault signal is represented with the application of DWT. Moreover, for fault signal processing, a set of high pass filters (HPF) and low pass filters (LPF) are employed, with the former handling low frequency domain signal analysis, while the latter handling high frequency domain signal analysis. Consequently, fault signal gets disintegrated into approximation (App)

coefficient [representation of large and small scale frequency components] and detail (Det) coefficient [representation of small and large-scale frequency components]. DWT decomposition tree is created as a result of App coefficient replication, as seen in Figure 3.

The occurrence of fault alters wavelet coefficients of waveforms, and these changes are also documented for a variety of other system parameters that contain crucial fault signature data. The expression for evaluating energy of a signal is given as (1).

$$E_i = \sum_{j=1}^n d_{ik}^2 \tag{1}$$

Where, the Det coefficient of a signal is specified as  $d_{ik}$ , number of points for wavelet coefficients  $j = 1, 2, \dots, n$  and scale  $i = 1, 2, \dots, l$ . With the occurrence of a fault or other transient events, the signal energy changes in line with the variation in the wavelet coefficient. The required input features for presented fault detection and classification model are obtained by evaluating the signal energy of every  $3\Phi$  signals. The DWT applied to a signal  $x$  at scale  $m$  and position  $n$  is (2).

$$DWT_{x,m,n} = \frac{1}{\sqrt{a_0^m}} \sum_l x(k) \psi^* \left( \frac{n-l a_0^m b_0}{a_0^m} \right) \tag{2}$$

Where,  $a_0^m$  specifies scale shift parameter,  $l a_0^m b_0$  specifies the time shift parameter, and the terms  $m$  and  $l$  are integer variables.

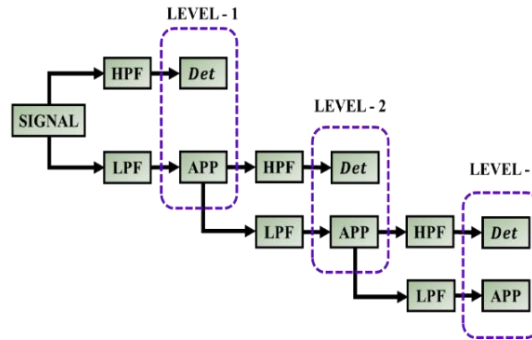


Figure 3. DWT decomposition tree

**4.3. CNN based fault classification**

The network fault types are classified with the aid of CNN and for the CNN to function, the fault signals are required to be converted to images, which is accomplished with the aid of wavelet-based signal analyser of MATLAB. The topology of the CNN as seen in the Figure 4 entails a softmax layer, max pooling, input layer along with fully connected layers and convolutional layers. They are mainly applied for 2D image recognition, since they are highly efficient when operated with image inputs. In addition to classification, the different layers found in CNN are also capable of performing architecture size reduction and feature extraction. The prominent features of the input image are extracted by convolution layer of CNN. Moreover, training of CNN is carried out by updating a collection of filters that estimates the dot products between input and filter values by spatially sliding across the input matrix. When these filters slide along the height and width of the image input, a 2D activation map is generated, which at each spatial position, provides the filter response.

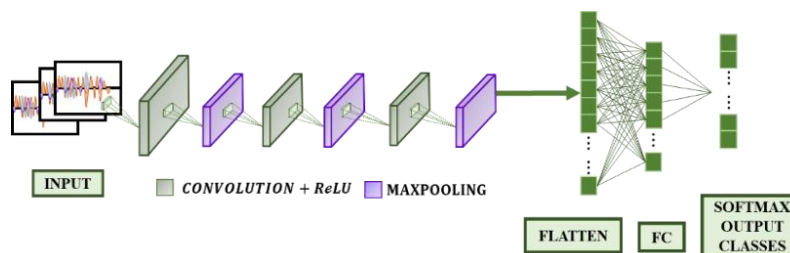


Figure 4. Architecture of CNN fault classifier

When the filters come across unique features in an input image like colours or edges, it gets activated and the network is also alerted. The max-pooling layer located between the convolutional layers, reduces overfitting by decreasing the parameters and size of the input image. The major process of classification in CNN takes place in the fully connected layer, which comprises of several neurons that are connected to the previous layer activation functions. The ReLU activation function applied at each convolution unit is (3).

$$f(z^l) = \begin{cases} z^l, & \text{if } z^l \geq 0 \\ 0, & \text{otherwise} \end{cases} \quad (3)$$

Where, the  $l$ th convolutional layer output element is specified as  $z^l$ . As mentioned earlier, the maxpooling layer, aids with the reduction of the overall computational complexity by minimizing the spatial size of parameters and features of the input data. All the pooled features are then converted to 1D vector by the flatten function. On the basis of features collected by the prior layers, the fully connected layer forms a new feature map. The final layer of the CNN is the softmax layer and for  $M$  classes, the output is given as (4).

$$z = [z_1, \dots, z_M]^T = \sigma(h) \quad (4)$$

Here, the type of fault determined in the  $m$ -th category of  $M$  classes is referred as  $z_M$ , the softmax function is specified as  $\sigma(h)$  and for the final fully connected layer  $h = [h_1, \dots, h_M]^T$ , the output is given as (5).

$$z_m = [\sigma(h)]_m = \frac{e^{h_m}}{\sum_{j=1}^M e^{h_j}} \quad (5)$$

With the aid of training data set  $V$ , CNN parameters are developed with the intention of minimizing the loss function. Here, the  $i$ th training sample's loss function is the cross entropy between the target and prediction, as in (6).

$$\text{Loss}(z^{(i)}) = -\sum_{m=1}^M t_m^{(i)} \log(z_m^{(i)}) \quad (6)$$

Where, for the  $i$ th training sample, if the index of ground truth is  $m$ , then  $t_m^{(i)} = 1$  or otherwise  $t_m^{(i)} = 0$ . The total training set loss is given as (7).

$$I(\theta) = \frac{1}{|V|} \sum_{i \in V} \text{Loss}(z^{(i)}) \quad (7)$$

Where, the test set elements are specified as  $|\cdot|$ . Moreover, in order to minimize the loss function, Adam optimizer is selected. An image of size  $224 \times 224 \times 3$  which represents the  $3\Phi$  voltage or current is provided as the CNN input. This image is accepted by the input layer, then it passes through the various filters of the convolution layer. It then subsequently passes through ReLU and maxpooling layer. Moreover, input data is down sampled by the pooling layer, in order to minimize overfitting. The convolution between the input matrix and filters is the major task performed by the convolution layer and its working is greatly influenced by the filter size. The smaller filter size leads to information loss, whereas a larger filter size leads to computational complexity. The presented fault classification technique is implemented in a hybridized power system encompassing wind and PV with individual control approaches, which are detailed as follows:

#### 4.4. PV system modelling

The PV cell circuit as seen in the Figure 5 is represented as a single diode model for the ease of understanding. The terms  $I_0$  and  $I_{ph}$  represents the diode saturated current and the photo generated current respectively, while the terms  $R_p$  and  $R_s$  refers to the shunt and series resistance respectively. Moreover, output current of PV cell is given as (8).

$$I_{PVcell} = I_{ph} - \left( I_0 (e^{V_D/\alpha V_T} - 1) \right) - \frac{V_{PVcell} + I_{PVcell} R_s}{R_p} \quad (8)$$

The output current of a PV module produced by combining multiple PV cells is shown as (9).

$$I_{PV} = I_{ph} - I_0 \left[ \exp \left( \frac{q(V_{PV} + I_{PV} R_s)}{AKT N_s} \right) - 1 \right] - \frac{V_{PV} + I_{PV} R_s N_s}{R_p N_s} \quad (9)$$

Where, the terms  $T, q, k$  and  $A$  refers to the operating temperature, electron charge, Boltzmann constant and diode ideality factor respectively. Moreover, the number of cells that together constitute a PV module is specified as  $N_s$ .

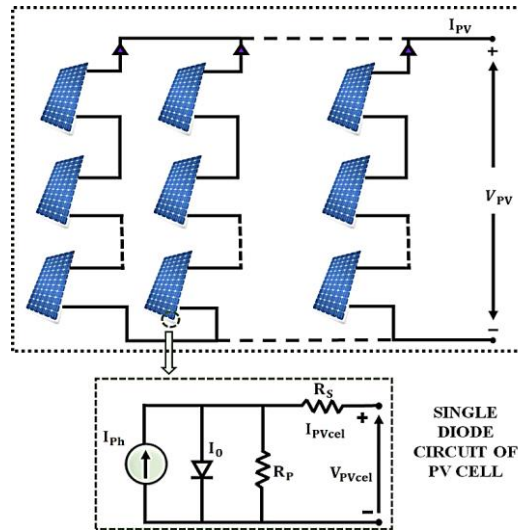


Figure 5. Configuration of a PV module and a PV cell

**4.5. Boost converter modelling**

The boost converter aids with maximizing the solar power generation  $P_{PV}$  by varying output voltage  $V_{PV}$  of PV array. The input voltage to converter is  $V_{PV}$ ,  $i_L$  represents the inductor current and  $V_{out}$  indicates the voltage output. Input capacitor which is shunt coupled to the PV generator is eliminated as seen in Figure 6, for simplifying the designing process of the MPPT controller.

On considering the continuous conduction, the boost converter operates in two switching modes, which are:

- On-state dynamics: In case of switch ON condition, the dynamics of output voltage and input current is expressed as (10).

$$\begin{cases} \frac{dI_{PV}}{dt} = \frac{V_{PV}}{L} \\ \frac{dV_{out}}{dt} = \frac{-V_{out}}{RC} \end{cases} \tag{10}$$

- Off-state dynamics: In case of switch OFF condition, the boost converter’s state space equation is given as (11).

$$\begin{cases} \frac{dI_{PV}}{dt} = \frac{V_{PV}-V_{out}}{L} \\ \frac{dV_{out}}{dt} = \frac{I_{PV}}{C} - \frac{V_{out}}{RC} \end{cases} \tag{11}$$

A time invariant nonlinear system is represented generally as (12).

$$\dot{X} = f(X) + g(X)u \tag{12}$$

Where,  $u \in [0 \ 1]$  and the vector state space is represented as  $X = [x_1 \ x_2 \ \dots \ x_n]^T$ . On the basis of (12), the model of boost converter is formulated by multiplying the duty cycle  $D$  with (10) and  $(1-D)$  with (11). Moreover, the state-space average approach is also used, in which (13) and (14).

$$D \in [0 \ 1] \tag{13}$$

$$X = [I_{PV} \ V_{out}]^T \tag{14}$$



In continuous mode, the boost converter model is given as (15).

$$\begin{cases} \frac{dI_{PV}}{dt} = \frac{V_{PV}}{L} - \frac{V_{out}}{L}(1 - D) \\ \frac{dV_{out}}{dt} = \frac{-V_{out}}{RC} + \frac{I_{PV}}{C}(1 - D) \end{cases} \quad (15)$$

The extracted power from the PV is further maximized with the aid of an appropriate MPPT approach. Here, a CFCLC is utilized as MPPT controller, which adjusts D of boost converter to allow extraction of maximum power.

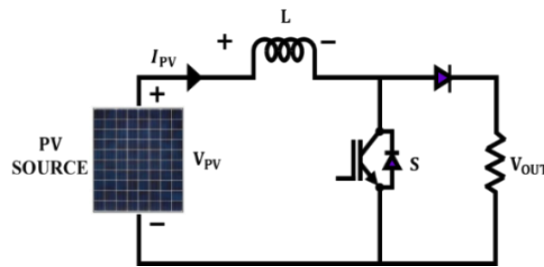


Figure 6. Boost converter without input capacitor

**4.6. CFCLC MPPT technique**

The fuzzy logic controller (FLC) is an effective mathematical tool capable of handling vague, unclear, uncertain and imprecise data. The mapping of the input to the output is carried out with the aid of if-then rules in an FLC and the term rule base refers to the collection of these if-then rules. The complexity of the rule base has a significant impact on the FLC's performance because a more complicated rule base necessitates a longer execution time. Thereby, with the aim of reducing the rule base complexity, a cascading approach is proposed for FLC in this work. The cascading technique is implemented by connecting several FLCs in series, with the output from one FLC serving as input to the following FLC. The CFCLC is used as an MPPT controller and the inputs to the MPPT are solar irradiance, temperature, \$V\_{PV}\$, \$I\_{PV}\$ and \$P\_{PV}\$. For a normal FLC with \$n\$ membership functions and \$m\$ inputs, the total number of rules is expressed as (16).

$$\text{Total number of rules} = m^n \quad (16)$$

As mentioned above, five inputs are considered for the MPPT controller. Thus, it is resulting in the requirement of \$5^5 = 3125\$ rules, in case of a normal FLC with five membership functions. However, in case of CFCLC MPPT as seen in Figure 7, requires a total of \$5^2 + 5^2 + 5^2 + 5^2 = 100\$ rules, thus successfully reducing the computational complexity of the MPPT controller.

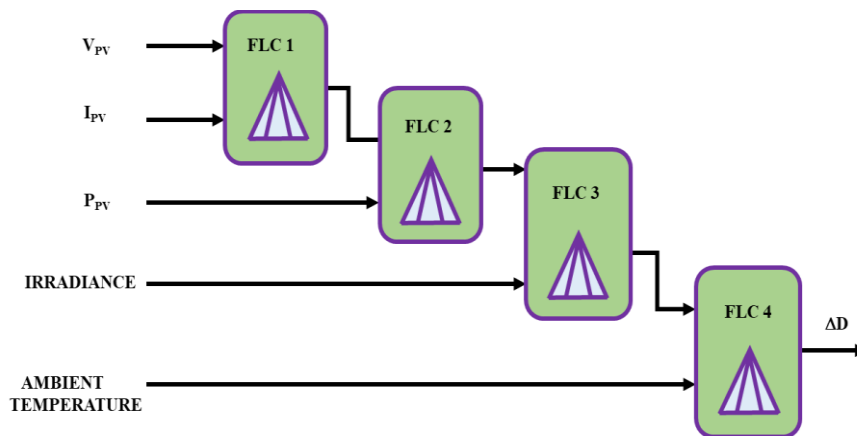


Figure 7. Structure of CFCLC MPPT

The FLC being an intelligent technique, is tuned on the basis of human experience and knowledge about the working of the system. Moreover, compared to conventional MPPT techniques, it overcomes the

problem of overshoot and is capable of maintaining the operating point at MPP in spite of fluctuations in temperature and irradiance. The inputs of the FLC are mapped to the fuzzy variable in the fuzzification block. The actual expert data are presented in the inference block through the membership rules contained in if-then statements. The linguistic inference rules are then converted to crisp numerical values in the output defuzzification block. In case of CFLC MPPT, the change in duty ratio command for the boost converter is attained as output.

#### 4.7. Modelling of DFIG based WECS

The characteristics of a wind turbine, which generates mechanical energy through the conversion of kinetic energy of the wind is given as (17)-(19).

$$\lambda_i = \frac{1}{1/\lambda + 0.08\beta - 0.035/(\beta^3 + 1)} \quad (17)$$

$$C_p(\lambda, \beta) = 0.645 \left( \frac{116}{\lambda_i} - 0.4\beta - 5 \right) e^{-21/\lambda_i} \quad (18)$$

$$T_m = \frac{0.5\rho\pi R^2 C_p(\lambda, \beta) V_{wind}^3}{\omega_{WT}} \quad (19)$$

Where, the terms  $\rho$ ,  $\beta$ ,  $\lambda$ ,  $C_p$  and  $R$  refers to the air density, pitch angle, tip speed ratio, power coefficient and blade radius respectively. A highly efficient AC asynchronous variable-speed generator with decreased mechanical stress, greater energy harvesting, and improved reactive power controllability is known as the DFIG. Figures 8(a) and (b) illustrate the structure and equivalent circuit of a DFIG. The DFIG is modelled with the aid of subsequent expressions. The stator voltage is estimated using (20).

$$\bar{v}_s = -R_s \bar{i}_s + \frac{1}{\omega_b} \frac{d\bar{\Psi}_s}{dt} + j \frac{1}{\omega_b} \frac{d\theta_s}{dt} \bar{\Psi}_s \quad (20)$$

The rotor voltage is expressed as (21), the stator flux linkage is expressed using (22), while the electromagnetic torque is expressed as (23).

$$\bar{v}_r = -R_r \bar{i}_r + \frac{1}{\omega_b} \frac{d\bar{\Psi}_r}{dt} + j \frac{1}{\omega_b} \frac{d\theta_r}{dt} \bar{\Psi}_r \quad (21)$$

$$\bar{\Psi}_s = L_s (-\bar{i}_s + \bar{i}_r), \bar{\Psi}_r = \bar{\Psi}_s + L_{kr} \bar{i}_r \quad (22)$$

$$t_e = -\text{Im}(\bar{\Psi}_s \bar{i}_r), p_s = -\text{Re}(\bar{v}_s \bar{i}_s) \quad (23)$$

Where the stator voltage, current, inductance and resistance are specified as  $v_s$ ,  $i_s$ ,  $L_s$  and  $R_s$  respectively, while the rotor voltage, current, inductance and resistance are specified as  $v_r$ ,  $i_r$ ,  $L_r$  and  $R_r$  respectively. The positive torque is specified as  $t_e$ , while the rotor and stator flux are designated as  $\Psi_r$  and  $\Psi_s$  respectively. To obtain a DC voltage output, a PWM rectifier is linked to the DFIG-based WECS's output. The PWM rectifier's output is stabilized using the PI controller, which provides the appropriate error compensation.

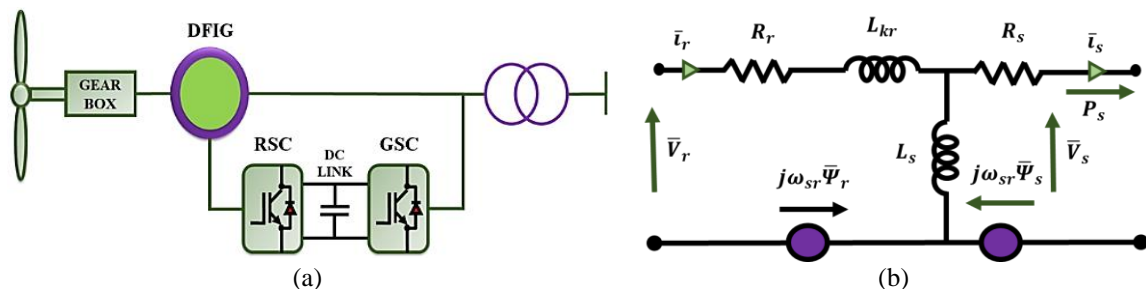


Figure 8. DFIG topology: (a) DFIG structure (b) DFIG equivalent circuit

## 5. RESULTS AND DISCUSSION

The process of fault detection using CNN classifier and DWT is proposed. The proposed fault detection scheme is considered in hybrid power system comprising of RES such as WECS and PV. Since both these RES

are characterized with intermittency, individual control methodologies are employed for stabilizing their outputs. Through accurate detection and correction of faults, the PQ of the entire system is enhanced. Moreover, by taking suitable maintenance measures, the breakdown of the entire power distribution system is also prevented. The simulation setup of suggested work is presented in Figure 9. The system includes a combination of WECS and a PV system, where the PV system incorporates a boost converter and a closed-loop CFLC MPPT for optimal power extraction. The output from the DFIG undergoes transformation through a PWM rectifier, controlled by a PI controller. Both the PV system and DFIG are linked to grid via a three-phase VSI. Continuous monitoring of voltage and current signals enables prompt fault detection. In the event of a fault, the signals are processed through DWT and the extracted features are input into a CNN classifier for rapid and accurate fault classification. The processing of signals is added as sub blocks in the simulation setup. This setup aims to expedite fault identification, allowing for timely maintenance actions to prevent PQDs and ultimately ensuring power system reliability, particularly in the context of intermittent and variable RES integration.

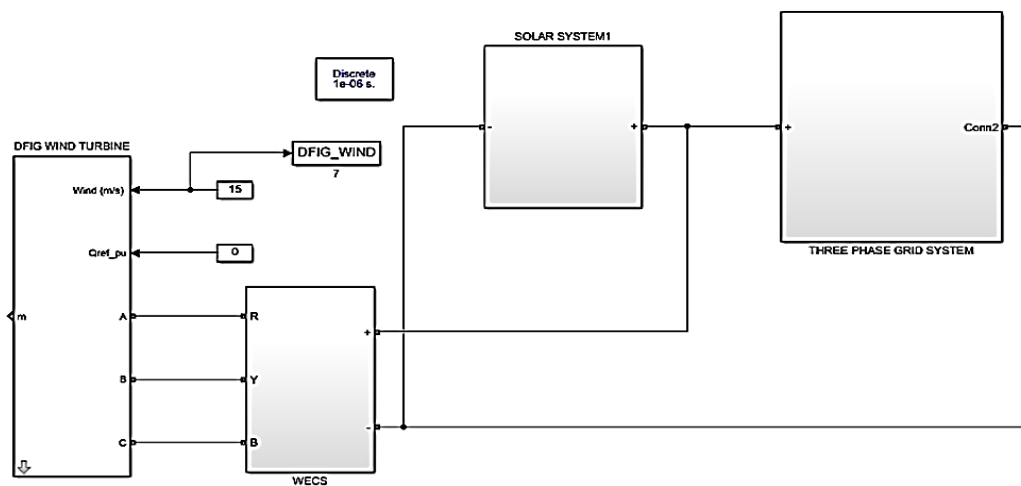


Figure 9. Simulation setup of the proposed work

### 5.1. Simulation results

The overall fault detection system is analysed on the basis of the simulation outcome derived from MATLAB. A simulation model for the suggested DWT-CNN based fault identification approach is developed and tested for its effectiveness in maintaining PQ in a power distribution system. Table 2 also includes a tabulation of the parameters for the developed simulation model.

The PV system unlike the conventional fossil fuel-based power systems, delivers a variable voltage supply as output. The PV panel output voltage waveform given in Figure 10(a), indicates that a rise in voltage level from 185 V to 195 V is observed at 0.2 s. This variation in voltage level is attributable to the operating condition changes such as variation in ambient temperature or solar irradiance. However, on the basis of the boost converter output voltage waveform shown in Figure 10(b), it is observed to maintain a 600 V at 0.2 s regardless of the input voltage fluctuation. This is mainly due to the effectiveness of the CFLC MPPT and the boost converter.

The waveform representing the DFIG voltage output is given in Figure 11(a). It is evident that the voltage output ranges at +600 V to -600 V and this AC voltage is then supplied to the PWM rectifier. The PWM rectifier is effective in delivering a stabilized DC voltage of 600 V as output from 0.15 s, with the assistance of PI controller as shown in Figure 11(b). The outputs showcasing the turbine rotor speed and torque are provided in Figure 12. The three currents of the three phases of the stator are provided in Figure 13.

DC-link voltage is noted to be a stable 600V from 0.075s after initial variations as seen in Figure 14. In a power distribution system, the abrupt addition or removal of loads induces PQDs such as voltage swell and sag as displayed in Figure 15. Voltage swell issue is characterized with instantaneous increase in voltage level, whereas the issue of voltage sag is characterized with instantaneous decrease in voltage level. Both these PQDs are required to be detected and compensated swiftly for ensuring the stable power distribution system working.

Here, PI controller and dq theory aids with the achievement of grid voltage synchronization and a stable voltage and current of range -400 V to +400 V and -13.5 A to +13.5 A respectively are maintained as seen in Figure 16(a)-(b). For better understanding, the phase A waveform of both grid voltage and current are considered as illustrated in Figure 16(c).

Table 2. Parameter specifications

Parameters	Values	Parameters	Values
No. of series cells	36	Operating voltage and current	16.8 V and 5.8 A
No. of panels	10	Switching frequency	1 kHz
DC-link voltage	600-1500 V	Load type	Variable
Area of each cell	125×31.25 mm		

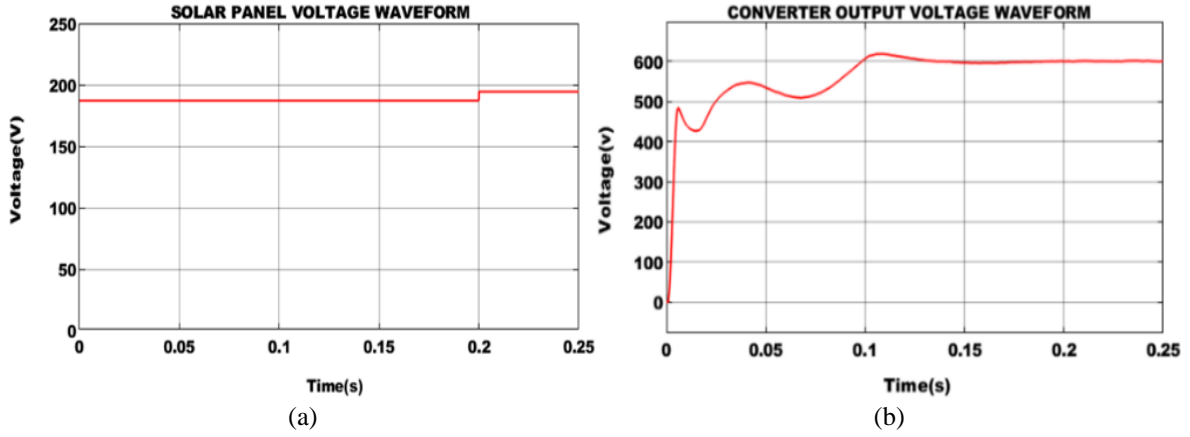


Figure 10. Output voltage waveforms: (a) PV panel and (b) boost converter

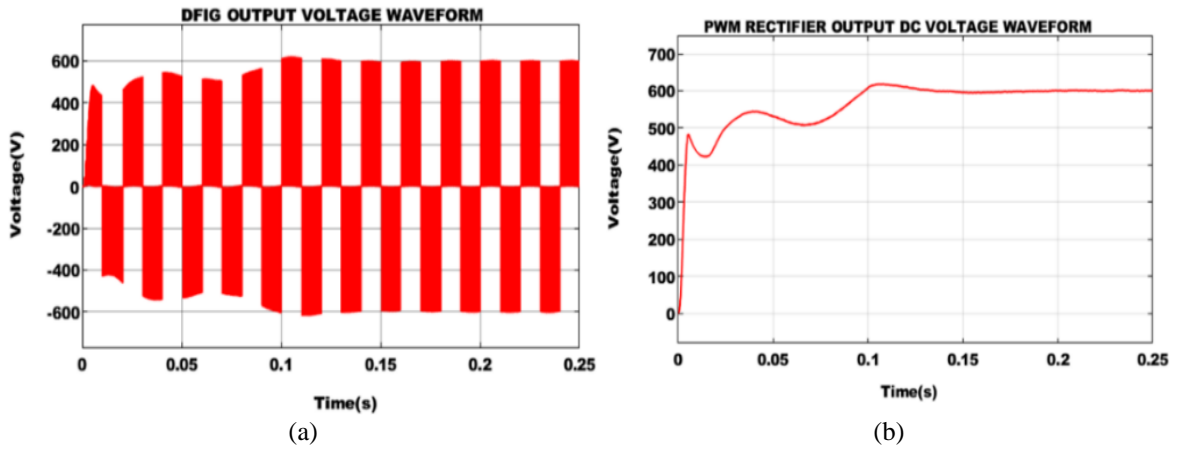


Figure 11. WECS waveforms representing: (a) DFIG output and (b) PWM rectifier

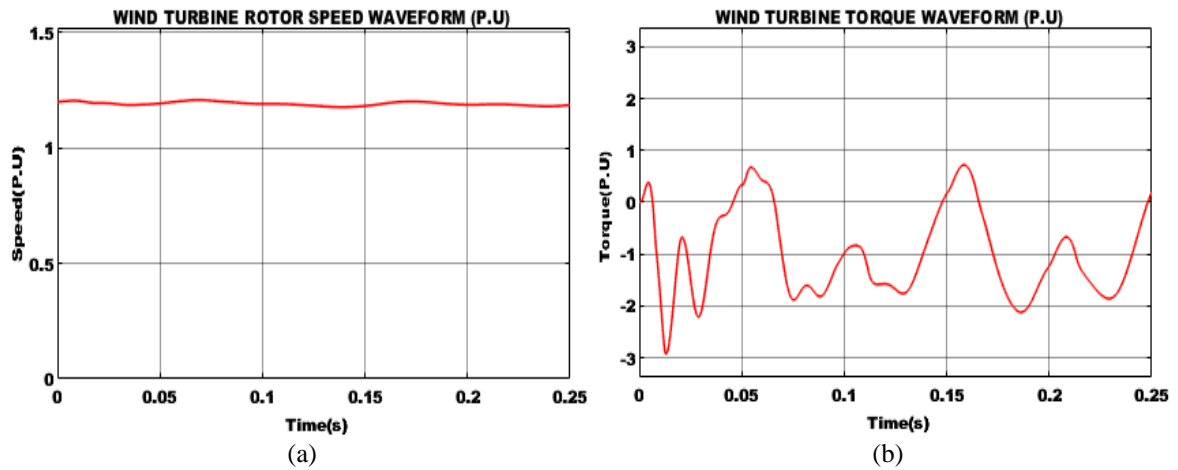


Figure 12. Waveforms showcasing wind turbine: (a) rotor speed and (b) torque

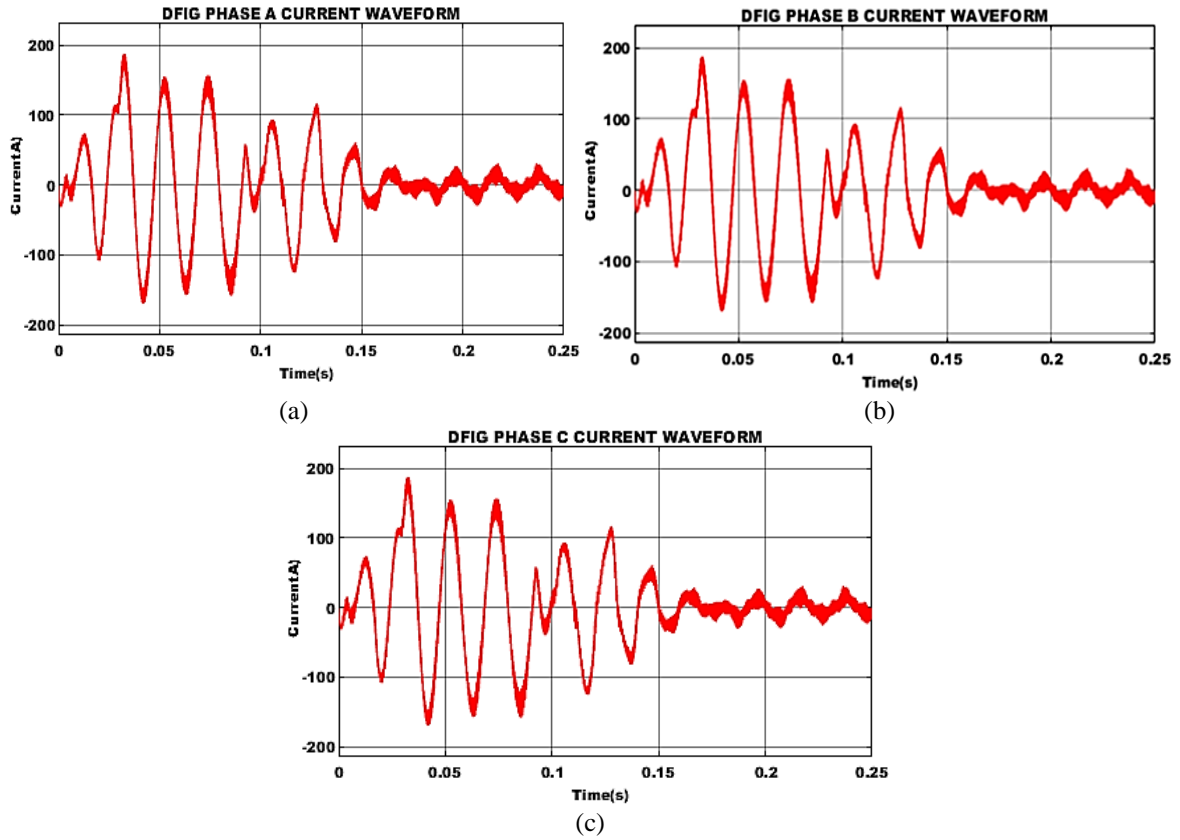


Figure 13. Output Waveforms of DFIG current: (a) phase A current, (b) DFIG phase B current, and (c) DFIG phase C current

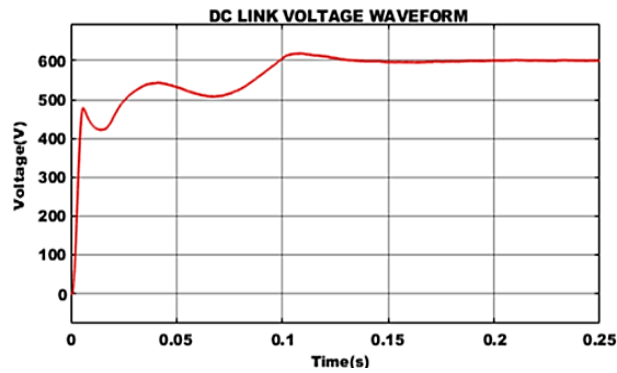


Figure 14. DC link voltage

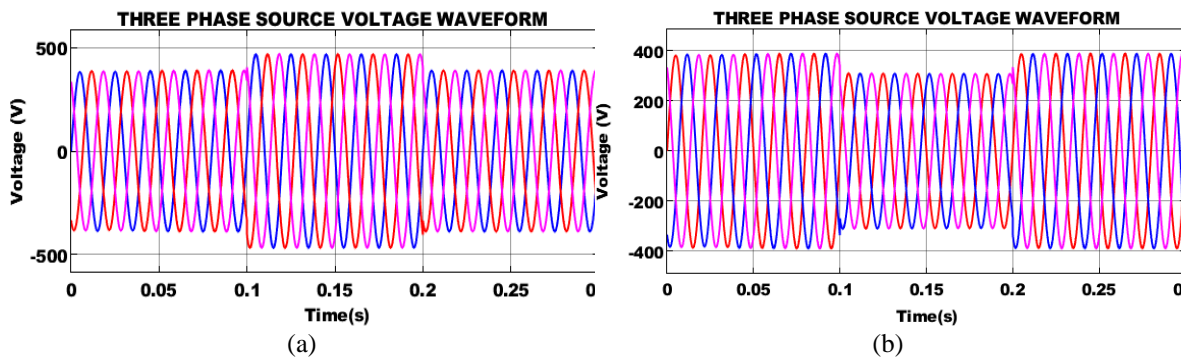


Figure 15. Source voltage affected by PQ issues of (a) voltage swell and (b) voltage sag

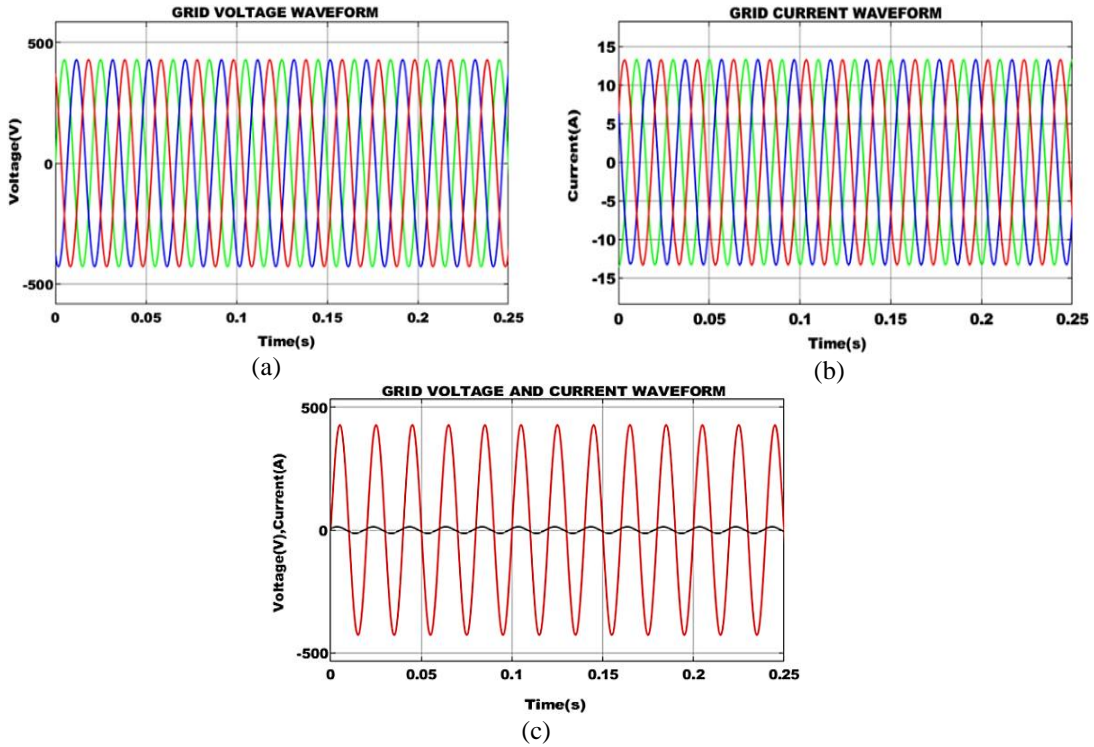


Figure 16. Grid side waveforms representing (a) voltage, (b) current, and (c) voltage and current waveform

Magnitude of real power as observed from Figure 17(a) is 8500 W, while the reactive power is noted to be below -150 VAR as seen in Figure 17(b). Since, both voltage and current waveforms are in phase, a power factor value of one is observed in Figure 17(c). The power factor value of one also implies that the amount of harmonic content in the grid side is very low. This is confirmed with the assistance of the THD waveform given in Figure 18, which shows that the value of THD is 0.89%.

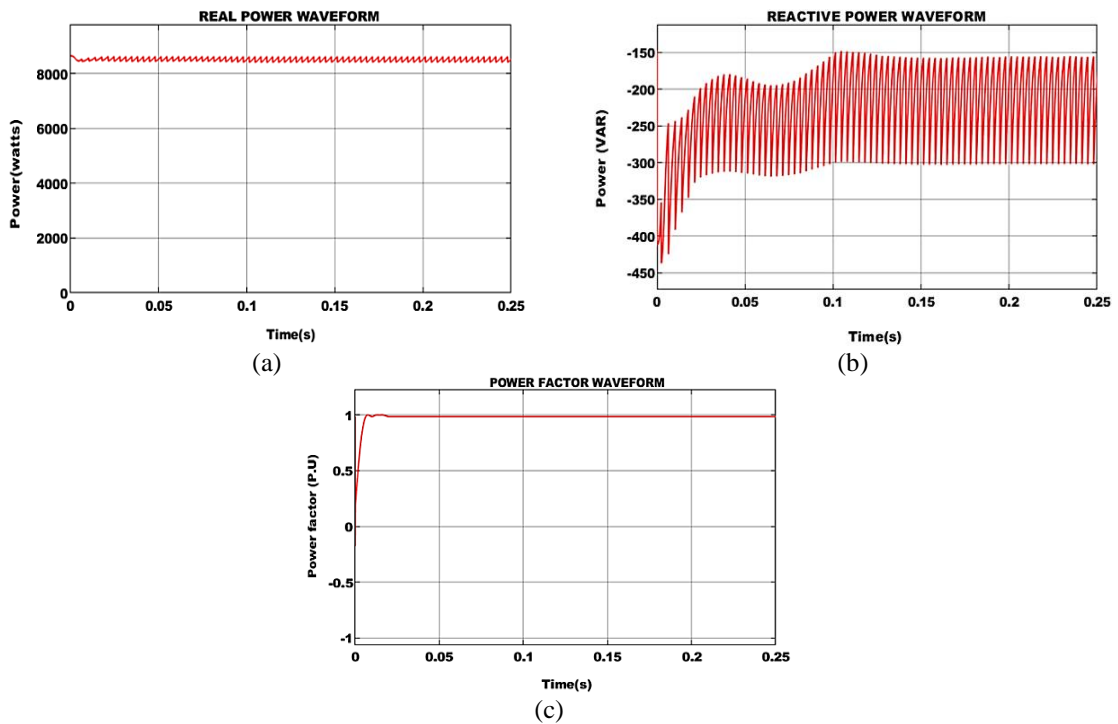


Figure 17. Grid side: (a) real power waveform, (b) reactive power waveform, and (c) power factor waveform

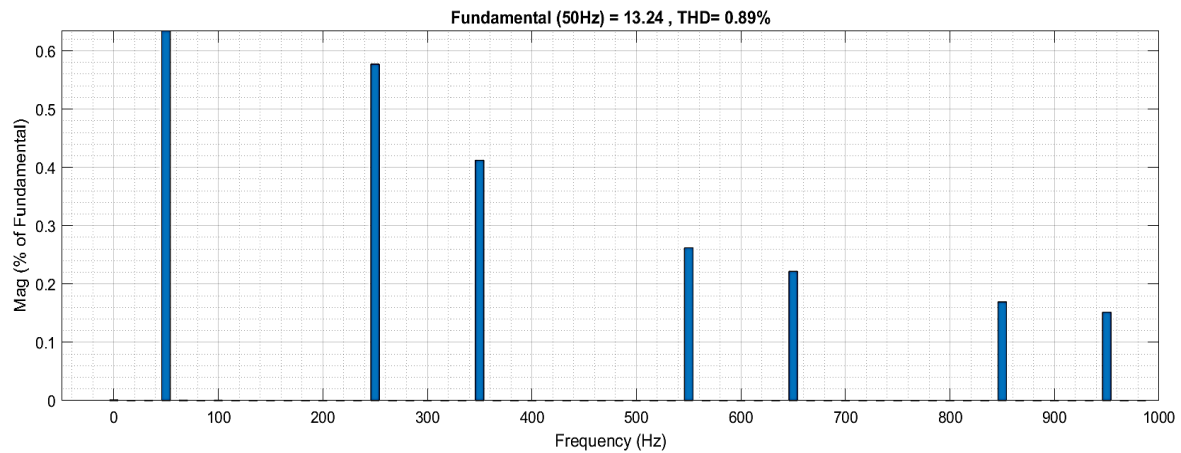


Figure 18. THD waveform

## 5.2. Fault analysis

The proposed fault detection system comprising of DWT and CNN classifier, undergoes a comprehensive evaluation under conditions simulating half the normal load to assess its fault detection capabilities across a variety of fault scenarios. This methodical analysis aims to validate the robustness and sensitivity of the system when the electrical system is not operating at full capacity. It is crucial for understanding its performance under less-than-ideal conditions.

### 5.2.1. Islanding condition

Islanding is an unsafe and critical condition during which the RES based distributed generators continues to supply power even when there is no power from the grid. The problem of islanding is dangerous to the utility workers and it causes damage to the customer appliances and inverters. Hence, the earliest detection of islanding is considered important.

The CNN classifier detects the islanding condition on the basis of grid current and voltage waveforms given in Figure 19. An abrupt variation in grid voltage is noted during the islanding condition that occurs between 0.5 to 0.6 seconds. The grid current remains unchanged, however a corresponding variation in real power and reactive power is observed during this time interval.

### 5.2.2. Line-to-ground fault

This fault typically arises from incidents such as a tree collapsing onto the power line, especially during periods of heavy rainfall. This fault condition materializes when the power line makes contact with the ground or comes into connection with the neutral line due to external factors like adverse weather conditions. Specifically, if the line physically descends to the ground or establishes contact with the neutral line, it results in what is referred to as a line-to-ground fault. This fault scenario can be triggered by a variety of environmental factors, with the consequences analyzed based on the extent and nature of the fault occurrence.

CNN classifier detects this fault on basis of current and voltage waveform displayed in Figure 20. The Line-to-Ground fault is observed between 0.5 to 0.6 seconds, during which the grid voltage witnesses a slight dip in its magnitude, while the grid current undergoes rapid distortions. Similarly, the active power also decreases in its value, whereas the reactive power experiences fluctuations during the occurrence of this fault.

### 5.2.3. Line-to-line fault

In a triphasic system, an asymmetrical fault arises when a short circuit arises between lines, termed as line-to-line fault. This type of fault manifests when an unintended connection or disruption arises between two distinct phases within the power distribution network. The line-to-line fault is characterized by a disruption in the equilibrium of the electrical system, leading to distinctive alterations in grid voltage and current. This fault condition occurrence can be attributed to various factors, such as equipment malfunction or external disturbances. The unsymmetrical nature of the fault introduces complexities in the electrical parameters, requiring a meticulous analysis for accurate detection and subsequent corrective measures. The recognition of line-to-line faults is pivotal in maintaining the integrity of the power system, as prompt identification enables swift intervention to prevent cascading failures and minimize potential damage to connected equipment.

The line-to-line fault is detected between 0.5 to 0.6 seconds by the CNN classifier. As seen in Figure 21, grid voltage is almost zero and grid current is affected by heavy distortions during this fault condition. The reactive power experiences a sudden increase, while the active power drops to zero. The CNN

classifier's performance is analyzed on the basis of accuracy, sensitivity and specificity in Figure 22(a) and it is observed that the CNN classifier outshines the functioning of all the other existing classifiers in these categories. It offers an excellent accuracy of 96.33% with sensitivity and specificity of 96%, which is comparatively better than the performance of ANN classifier as seen in Table 3. Moreover, the efficiency of the proposed CFLC MPPT is 91% as given in Figure 22(b). Table 4 presents a comprehensive comparison of the performance of various fault detection systems under diverse fault conditions. The proposed CNN exhibits an overall accuracy of 96.33%, which is significantly greater than the average accuracy of other models (ranging from 84% to 92%). This emphasizes the comprehensive effectiveness of the CNN-based approach across different fault conditions.

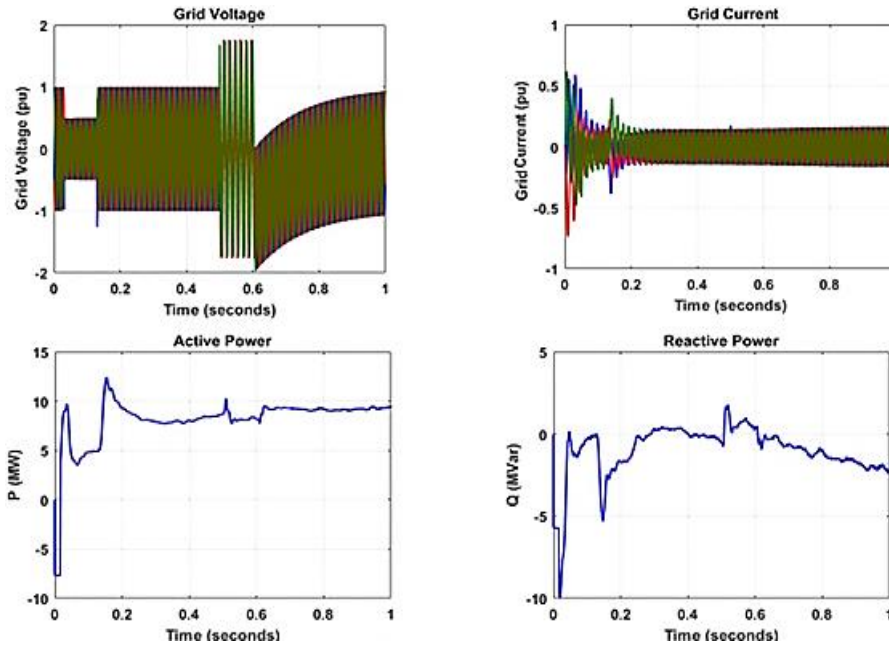


Figure 19. Islanding condition waveforms

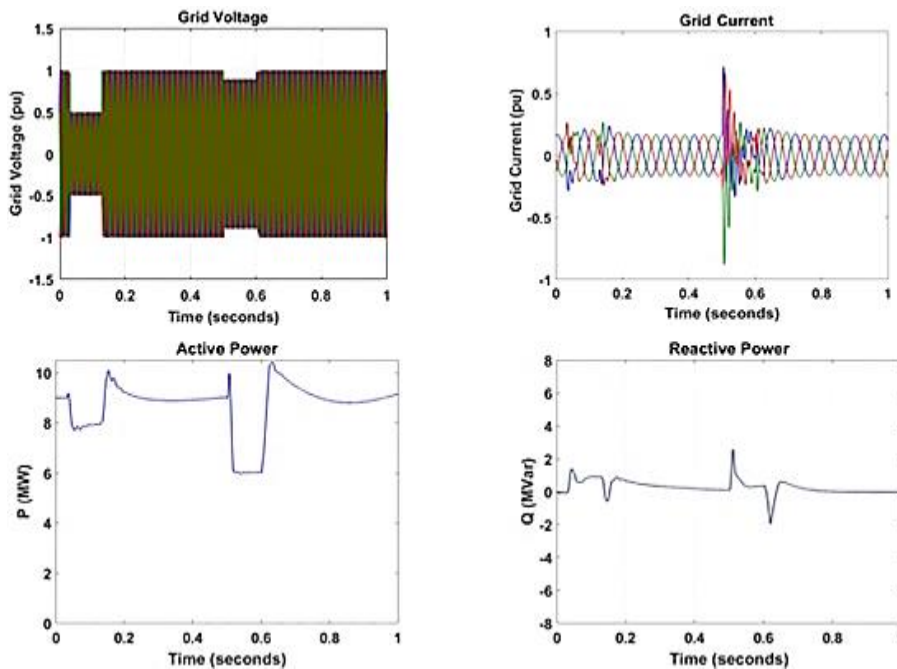


Figure 20. Parameters noted in case of line-to-ground fault



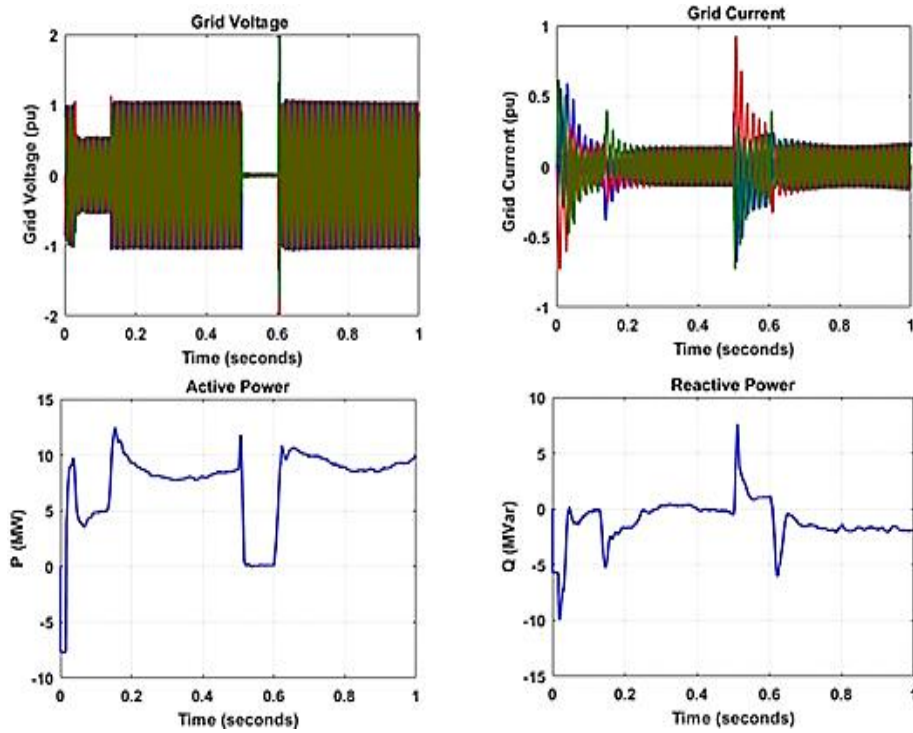


Figure 21. Parameters noted in case of line-to-line fault

Table 5 offers a comparative overview of the classifiers based on their training time, inference speed, and resource utilization, providing insights into the efficiency and computational demands of each model. The proposed CNN exhibits a training time of 10.5 hours, an inference speed of 5 milliseconds, and a resource utilization of 85%. These metrics collectively demonstrate the efficiency and computational effectiveness of the proposed approach in training the model, making rapid predictions during inference, and utilizing system resources optimally. In comparison, the DT classifier demonstrates a shorter training time of 2.3 hours but with a slightly higher inference speed of 15 milliseconds and a resource utilization of 70%. SVM, RF, and FNN show varying performance across these metrics, while the ANN classifier requires the longest training time (20.1 hours) with moderate inference speed (12 milliseconds) and resource utilization (60%). These results provide valuable insights into the trade-offs between training time, inference speed, and resource utilization for each classifier. The proposed CNN stands out for achieving a balanced performance across these metrics, showcasing its suitability for real-time fault detection applications in power systems.

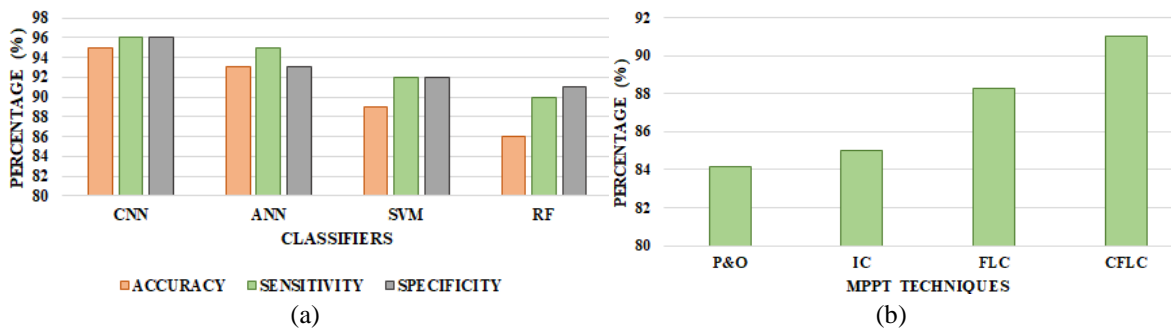


Figure 22. Comparison charts for (a) classifiers and (b) efficiency

Table 3. Comparison of CNN against ANN classifier

Classifiers	Accuracy	Sensitivity	Specificity
ANN	87%	95%	93%
CNN	96.33%	96%	96%

Table 4. Fault detection system performance comparison under various fault conditions

Fault condition	CNN	DT	SVM	RF	FNN	ANN
Islanding	98%	90%	92%	93%	94%	91%
Line-to-ground fault	95%	87%	88%	89%	92%	86%
Line-to-line fault	96%	85%	86%	87%	90%	84%
Overall accuracy	96.33%	87.33%	88.67%	89.67%	92%	87%

Table 5. Computational efficiency comparison of classifiers

Classifier	Training time (hrs)	Inference speed (ms)	Resource utilization
CNN	10.5	5	85
DT	2.3	15	70
SVM	8	8	80
RF	12.2	7	75
FNN	15.8	10	65
ANN	20.1	12	60

### 5.3. Discussions

The proposed fault detection system, integrating DWT and CNN, demonstrates notable effectiveness in enhancing the PQ and reliability of a hybrid power system comprising WECS and PV. The simulation results, conducted in MATLAB, provide insights into the system's performance under various conditions. The stability of both WECS and PV, achieved through individual control methodologies, ensures the system's resilience against faults and contributes to maintaining a stable PQ. The PV system, characterized by variable voltage output, exhibits stable voltage maintenance through the boost converter and CFLC based MPPT. Similarly, the WECS output is stabilized through a PI controller. The fault analysis, conducted under different conditions such as islanding, line-to-ground fault, and line-to-line fault, showcases the CNN classifier's robust performance, with an overall accuracy of 96.33%. The comparative analysis against other classifiers, including ANN, highlights the superiority of the proposed CNN classifier in terms of accuracy, sensitivity, and specificity. Additionally, the computational efficiency comparison reveals that the CNN model achieves a balanced performance with a training time of 10.5 hours, inference speed of 5 milliseconds, and resource utilization of 85%. The implications of these findings extend to the future development of fault detection systems in power distribution. The robustness demonstrated by the CNN classifier, coupled with efficient computational performance, positions it as a promising tool for real-time fault detection applications. This research contributes valuable insights into advancing power system stability and reliability in the context of increasing renewable energy source integration.

## 6. CONCLUSION




The increased penetration of RES in power system has resulted in the existence of severe protection issues, PQDs and faults. Therefore, to improve stability, PQ, and reliability of power system, these faults are required to be identified instantly without delay. So, a CNN classifier-based fault detection is proposed in this work for identifying faults taking place in a hybrid power system consist of wind and PV. Moreover, features of the fault signal are extracted with the aid of DWT. Furthermore, individual control approaches are applied for wind and PV for stabilizing their outputs. Consequently, a boost converter along with CFLC MPPT is employed for PV, while PI controller is employed for WECS. The MATLAB platform is utilized for carrying out the simulation of the proposed fault detection approach. Moreover, the classification capability of CNN is tested for various kinds of fault such as line-to-line fault, islanding and line-to-ground faults. On the basis of the obtained outcomes, the CNN classifier offers an exceptional classification accuracy of 96.33% and it outperforms other available classifiers such as ANN, SVM, and RF.

## REFERENCES




- [1] M. K. H. Rabaia *et al.*, "Environmental impacts of solar energy systems: A review," *Science of The Total Environment*, vol. 754, p. 141989, Feb. 2021, doi: 10.1016/j.scitotenv.2020.141989.
- [2] R. M. Elavarasan *et al.*, "A Comprehensive Review on Renewable Energy Development, Challenges, and Policies of Leading Indian States with an International Perspective," *IEEE Access*, vol. 8, pp. 74432–74457, 2020, doi: 10.1109/ACCESS.2020.2988011.
- [3] C. I. Garcia, F. Grasso, A. Luchetta, M. C. Piccirilli, L. Paolucci, and G. Talluri, "A Comparison of Power Quality Disturbance Detection and Classification Methods Using CNN, LSTM and CNN-LSTM," *Applied Sciences*, vol. 10, no. 19, p. 6755, Sep. 2020, doi: 10.3390/app10196755.
- [4] V. Babu, K. S. Ahmed, Y. M. Shuaib, and M. Mani, "A novel intrinsic space vector transformation based solar fed dynamic voltage restorer for power quality improvement in distribution system," *Journal of Ambient Intelligence and Humanized Computing*, 2021, doi: 10.1007/s12652-020-02831-0.

- [5] R. Eslami, S. H. H. Sadeghi, H. Askarian-Abyaneh, and A. Nasiri, "A Novel Method for Fault Detection in Future Renewable Electric Energy Delivery and Management Microgrids, Considering Uncertainties in Network Topology," *Electric Power Components and Systems*, vol. 45, no. 10, pp. 1118–1129, 2017, doi: 10.1080/15325008.2017.1292433.
- [6] Y. Zhang and W. Wei, "Decentralised coordination control strategy of the PV generator, storage battery and hydrogen production unit in islanded AC microgrid," *IET Renewable Power Generation*, vol. 14, no. 6, pp. 1053–1062, 2020, doi: 10.1049/iet-rpg.2019.0842.
- [7] G. Magdy, G. Shabib, A. A. Elbaset, and Y. Mitani, "A novel coordination scheme of virtual inertia control and digital protection for microgrid dynamic security considering high renewable energy penetration," *IET Renewable Power Generation*, vol. 13, no. 3, pp. 462–474, 2019, doi: 10.1049/iet-rpg.2018.5513.
- [8] A. Prasad, J. Belwin Edward, and K. Ravi, "A review on fault classification methodologies in power transmission systems: Part— I," *Journal of Electrical Systems and Information Technology*, vol. 5, no. 1, pp. 48–60, 2018, doi: 10.1016/j.jesit.2017.01.004.
- [9] S. G. Reddy, S. Ganapathy, and M. Manikandan, "Three Phase Four Switch Inverter Based DVR for Power Quality Improvement with Optimized CSA Approach," *IEEE Access*, vol. 10, pp. 72263–72278, 2022, doi: 10.1109/ACCESS.2022.3188629.
- [10] V. Babu, K. Shafeeqe Ahmed, Y. Mohamed Shuaib, and M. Manikandan, "Power Quality Enhancement Using Dynamic Voltage Restorer (DVR)-Based Predictive Space Vector Transformation (PSVT) with Proportional Resonant (PR)-Controller," *IEEE Access*, vol. 9, pp. 155380–155392, 2021, doi: 10.1109/ACCESS.2021.3129096.
- [11] E. Sortomme, S. S. Venkata, and J. Mitra, "Microgrid protection using communication-assisted digital relays," *IEEE Transactions on Power Delivery*, vol. 25, no. 4, pp. 2789–2796, 2010, doi: 10.1109/TPWRD.2009.2035810.
- [12] H. Al-Nasser, M. A. Redfern, and F. Li, "A voltage based protection for micro-grids containing power electronic converters," *2006 IEEE Power Engineering Society General Meeting, PES, 2006*, doi: 10.1109/pes.2006.1709423.
- [13] H. Al-Nasser and M. A. Redfern, "Harmonics content based protection scheme for micro-grids dominated by solid state converters," *2008 12th International Middle East Power System Conference, MEPCON 2008*, pp. 50–56, 2008, doi: 10.1109/MEPCON.2008.4562361.
- [14] A. Hooshyar, E. F. El-Saadany, and M. Sanaye-Pasand, "Fault Type Classification in Microgrids Including Photovoltaic DGs," *IEEE Transactions on Smart Grid*, vol. 7, no. 5, pp. 2218–2229, 2016, doi: 10.1109/TSG.2015.2451675.
- [15] A. Gururani, S. R. Mohanty, and J. C. Mohanta, "Microgrid protection using Hilbert-Huang transform based-differential scheme," *IET Generation, Transmission and Distribution*, vol. 10, no. 15, pp. 3707–3716, 2016, doi: 10.1049/iet-gtd.2015.1563.
- [16] T. Gush, S. B. A. Bukhari, K. K. Mehmood, S. Admasie, J. S. Kim, and C. H. Kim, "Intelligent fault classification and location identification method for microgrids using discrete orthonormal stockwell transform-based optimized multi-kernel extreme learning machine," *Energies*, vol. 12, no. 23, 2019, doi: 10.3390/en12234504.
- [17] Y. Y. Hong, Y. H. Wei, Y. R. Chang, Y. Der Lee, and P. W. Liu, "Fault detection and location by static switches in microgrids using wavelet transform and adaptive network-based fuzzy inference system," *Energies*, vol. 7, no. 4, pp. 2658–2675, 2014, doi: 10.3390/en7042658.
- [18] V. Le, X. Yao, C. Miller, and B. H. Tsao, "Series DC Arc Fault Detection Based on Ensemble Machine Learning," *IEEE Transactions on Power Electronics*, vol. 35, no. 8, pp. 7826–7839, 2020, doi: 10.1109/TPEL.2020.2969561.
- [19] F. Ye, Z. Zhang, K. Chakrabarty, and X. Gu, "Board-level functional fault diagnosis using multikernel support vector machines and incremental learning," *IEEE Transactions on Computer-Aided Design of Integrated Circuits and Systems*, vol. 33, no. 2, pp. 279–290, 2014, doi: 10.1109/TCAD.2013.2287184.
- [20] Y. Y. Hong and M. T. A. M. Cabatac, "Fault Detection, Classification, and Location by Static Switch in Microgrids Using Wavelet Transform and Taguchi-Based Artificial Neural Network," *IEEE Systems Journal*, vol. 14, no. 2, pp. 2725–2735, 2020, doi: 10.1109/JSYST.2019.2925594.
- [21] B. Padakanti, I. A. Chidambaram, and M. Mani, "An ANN Based MPPT for Power Monitoring in Smart Grid using Interleaved Boost Converter," *Tehnicki Vjesnik*, vol. 30, no. 2, pp. 381–389, 2023, doi: 10.17559/TV-20220820194302.
- [22] S. Mishra, C. N. Bhende, and B. K. Panigrahi, "Detection and Classification of Power Quality Disturbances Using S-Transform and Probabilistic Neural Network," *IEEE Transactions on Power Delivery*, vol. 23, no. 1, pp. 280–287, Jan. 2008, doi: 10.1109/TPWRD.2007.911125.
- [23] T. P. Kumar, S. Ganapathy, and M. Manikandan, "Improvement of voltage stability for grid connected solar photovoltaic systems using static synchronous compensator with recurrent neural network," *Electrical Engineering and Electromechanics*, vol. 2022, no. 2, pp. 69–77, 2022, doi: 10.20998/2074-272X.2022.2.10.
- [24] M. Shaik, A. G. Shaik, and S. K. Yadav, "Hilbert–Huang transform and decision tree based islanding and fault recognition in renewable energy penetrated distribution system," *Sustainable Energy, Grids and Networks*, vol. 30, 2022, doi: 10.1016/j.segan.2022.100606.
- [25] Z. El Mrabet, N. Sugunraj, P. Ranganathan, and S. Abhyankar, "Random Forest Regressor-Based Approach for Detecting Fault Location and Duration in Power Systems," *Sensors*, vol. 22, no. 2, 2022, doi: 10.3390/s22020458.
- [26] K. S. V. Swarna, A. Vinayagam, M. Belsam Jeba Ananth, P. Venkatesh Kumar, V. Veerasamy, and P. Radhakrishnan, "A KNN based random subspace ensemble classifier for detection and discrimination of high impedance fault in PV integrated power network," *Measurement: Journal of the International Measurement Confederation*, vol. 187, 2022, doi: 10.1016/j.measurement.2021.110333.
- [27] A. Eskandari, M. Aghaei, J. Milimonfared, and A. Nedaei, "A weighted ensemble learning-based autonomous fault diagnosis method for photovoltaic systems using genetic algorithm," *International Journal of Electrical Power and Energy Systems*, vol. 144, 2023, doi: 10.1016/j.ijepes.2022.108591.
- [28] T. Biswal and S. K. Parida, "A novel high impedance fault detection in the micro-grid system by the summation of accumulated difference of residual voltage method and fault event classification using discrete wavelet transforms and a decision tree approach," *Electric Power Systems Research*, vol. 209, 2022, doi: 10.1016/j.epr.2022.108042.
- [29] C. Li *et al.*, "Takagi–Sugeno fuzzy based power system fault section diagnosis models via genetic learning adaptive GSK algorithm," *Knowledge-Based Systems*, vol. 255, 2022, doi: 10.1016/j.knosys.2022.109773.
- [30] B. Xu, X. Yin, X. Yin, Y. Wang, and S. Pang, "Fault diagnosis of power systems based on temporal constrained fuzzy petri nets," *IEEE Access*, vol. 7, pp. 101895–101904, 2019, doi: 10.1109/ACCESS.2019.2930545.




**BIOGRAPHIES OF AUTHORS**

**Abdul Quawi**    graduated in B. Tech in Electrical and Electronics Engineering, M.Tech. in Electrical Power Engineering and pursuing Ph.D. Power Quality at B. S. Abdur Rahman Crescent Institute of Science and Technology-A deemed to be University, Chennai, Tamil Nadu, India. Presently, he is working as an electrical instructor in Maulana Azad National Urdu University Hyderabad, Telangana, India. He worked as assistant professor in Alhabeeb College of Engineering & Technology Hyderabad, Telangana, India from January 2013 to February 2015. He is having more than 8 years of teaching experience in the department of Electrical and Electronics Engineering. He can be contacted at email: quawiabdul@gmail.com.



**Y. Mohamed Shuaib**    graduated in B.E in Electrical and Electronics Engineering, M.E in Power Systems Engineering and Ph.D. in Electrical Engineering at Jawaharlal Nehru Technological University, Telangana, India in November, 2015. Presently, he is working as professor of the Department of Electrical and Electronics Engineering at B. S. Abdur Rahman Crescent Institute of Science and Technology-A deemed to be University, Chennai, Tamilnadu, India. He is having more than 20 years of teaching experience in the Department of Electrical and Electronics Engineering. His research area is power quality, power system. He can be contacted at email: mdshuaiby@crescent.education.



**M. Manikandan**    graduated in B.E in Electrical, M.E in Power Electronics and Drives. He was awarded Ph.D. in EEE at Anna University, Chennai. He is a member of IEE, ISTE and IAENG. He has published 17 papers in international and national level journals. Presently, he is working as professor of the Department of Electrical and Electronics Engineering at Jyothishmathi Institute of Technology and Science Karimnager, Telangana, India. He is having more than 17 years of teaching experience in the Department of Electrical and Electronics Engineering. His research area is power quality, power system. He can be contacted at email: cm.manikandan@gmail.com.